



The impact of traffic on air quality in Ireland: insights from simultaneous kerbside and sub-urban monitoring of submicron aerosols

5 Chunshui Lin^{1,2,3}, Darius Ceburnis¹, Wei Xu^{1,2}, Eimear Heffernan⁴, Stig Hellebust⁴, John Gallagher⁵, Ru-
Jin Huang^{1,2,3*}, Colin O'Dowd^{1*}, and Jurgita Ovadnevaite¹

¹School of Physics, Ryan Institute's Centre for Climate and Air Pollution Studies, National University of Ireland Galway, University Road, Galway. H91 CF50, Ireland

²State Key Laboratory of Loess and Quaternary Geology and Key Laboratory of Aerosol Chemistry and Physics, Institute of Earth Environment, Chinese Academy of Sciences, 710061, Xi'an, China

10 ³Center for Excellence in Quaternary Science and Global Change, Chinese Academy of Sciences, Xi'an 710061, China

⁴School of Chemistry and Environmental Research Institute, University College Cork, Cork, Ireland

⁵Department of Civil, Structural & Environmental Engineering, Trinity College Dublin, the University of Dublin, Ireland.

Correspondence to: Ru-Jin Huang (rujin.huang@ieecas.cn) and Colin O'Dowd (colin.odowd@nuigalway.ie)

Abstract: To evaluate the impact of traffic on urban air quality, the chemical composition and sources of submicron aerosols
15 (PM₁) were simultaneously investigated at a kerbside site in Dublin city centre and a residential site in sub-urban Dublin (~5 km apart) from 4 September to 9 November in 2018. Through the detailed comparison of one-week non-heating period in early September and heating period in late October, black carbon (BC) was found to be the most dominant component (38-55% or 5.6-7.1 μg m⁻³) of PM₁ at the kerbside while organic aerosol (OA) was the most important (46-63% of PM₁ or 1.0-8.7 μg m⁻³) at the residential site. The daily and weekly cycle of BC at the kerbside during non-heating period pointed to the major source
20 of vehicular emissions, consistent with that for nitrogen oxides (NO_x). However, traffic emissions were found to have a minor impact on air quality at the residential site due to its distance from traffic sources, as well as the effects of wind speed and wind direction. As a result of vehicular emissions and the street canyon effect, the kerbside increment (from urban background) ratio of up to 25:1 was found for BC during the non-heating period, but reduced to 10:1 during the heating period due to the additional sources of solid fuel burning impacting the air quality at both sites simultaneously. OA source analysis shows only
25 18-27% (0.9-1.2 μg m⁻³) of OA at the kerbside associated with vehicular emissions, with higher contributions from cooking (18-36% or ~1.2 μg m⁻³), solid fuel burning (~33% or ~2.1 μg m⁻³), and oxygenated OA (31-37% or 1.2-2.0 μg m⁻³). At the residential site, solid fuel burning contributed to approximately 50% (2.7 μg m⁻³) of OA during the heating period, while oxygenated OA accounted for almost 65% (0.5 μg m⁻³) of OA during the non-heating period. Based on simultaneous investigation of PM₁ at different urban settings (i.e. residential vs kerbside), this study highlights temporal and spatial
30 variability of sources within Dublin city centre and the need for additional aerosol characterisation studies to improve targeted mitigation solutions for greater impact on urban air quality. Moreover, traffic and residential heating may hold different implications for health and climate as indicated by the significant increment of BC at the kerbside and the large geographic impact of OA from residential heating at both the kerbside and residential sites.



1 Introduction

35 Aerosol particles adversely affect human health, causing morbidity and premature mortality (Pope III et al., 2002; Cohen et al., 2017; Burnett et al., 2018). In particular, urban areas are usually more polluted than rural areas due to the proximity to pollution sources including traffic, cooking, and various other activities such as residential heating. To make things worse, the street canyon effects in urban areas result in poor dispersion conditions, trapping the pollutants in downtown areas where the streets are flanked by buildings on both sides creating a canyon-like environment (Fuzzi et al., 2015). The term ‘urban
40 increment’ is defined as the increase in air pollution parameters in the urban background above the rural surroundings while ‘kerbside increment’ is defined as the increase in concentrations at a kerbside or street site relative to the urban background (Lenschow et al., 2001; Mues et al., 2013; Fuzzi et al., 2015). Models often underestimate the urban increment let alone kerbside increment, due to the poor grid resolution and not taking into account the urban micron-environment such as the urban canyon and urban heat-island effects (Mues et al., 2013). Therefore, field campaigns, especially those simultaneously
45 measuring at different settings (e.g., residential site vs. kerbside) in urban area, are required to study the spatial variation of aerosols and their sources as well as to provide constraints for the models.

Aerosol can be broadly categorized into two classes: primary and secondary (Fuzzi et al., 2015). Primary aerosols are directly emitted from their emissions sources such as traffic, cooking, and biomass burning while secondary aerosols are formed from their corresponding precursor gases (An et al., 2019). Primary aerosols often show enhanced concentrations when
50 close to their sources (e.g., at the kerbside), while secondary aerosols are more homogeneously distributed (Hallquist et al., 2009; Zhang et al., 2015; Gentner et al., 2017). Mohr et al. (2011) showed a kerbside increment of up to $11 \mu\text{g m}^{-3}$ for black carbon (BC) and $2.5 \mu\text{g m}^{-3}$ for hydrocarbon-like organic aerosol (HOA) at a road side in Zurich with the mobile measurements using an Aerosol Mass Spectrometer (AMS). While mobile or on-road measurements can provide a detailed characterization of the spatial variation of the chemical components and sources (e.g., traffic) of aerosols, mobile measurements can also be
55 strongly influenced by the emission from a specific source e.g., from an old type truck (or high emitters), not representing the average fleet (Fuzzi et al., 2015). Moreover, mobile measurements are usually conducted at a specific time of the day, failing to capture the temporal variation of aerosols over longer periods (e.g., days to months) (Mohr et al., 2011; Fuzzi et al., 2015). A fixed installation of instruments at multiple sites simultaneously can, therefore, provide more detailed information about both the temporal and spatial variation of aerosols. Crippa et al. (2013) investigated the temporal evolution of the submicron
60 aerosol at three sites (one urban centre and two urban background sites) in Paris during wintertime. In contrast to the finding by Mohr et al. (2011), Crippa et al. (2013) concluded that the submicron aerosol in Paris was dominated by regional transport and that the emissions from Paris itself had an insignificant impact on the urban backgrounds. The discrepancies between the individual studies may be related to the specific geographic environment and the periods of the measurement (Fuzzi et al., 2015).

65 Dublin, the capital city of Republic of Ireland in Western Europe, is home to ~1 million people. Previous study conducted at a suburban site in the residential area in Dublin has shown that air quality was strongly influenced by residential heating



sources in winter (Lin et al., 2018). However, the impact of traffic emissions on this residential site was shown to be minor probably due to the distance (~500 m) from the nearest roads, as well as the strict emission standard (Lin et al., 2018). The minor influence of traffic at the residential site was also shown in a west coast city of Galway in Ireland during both summer
70 (Lin et al., 2019a) and winter conditions (Lin et al., 2017). In particular, the diurnal pattern of HOA shows largely enhanced concentration in the evening when compared to that during the morning rush hours, suggesting residential heating is the major source of HOA in suburban Dublin (Lin et al., 2019b). Heating source of HOA is also reported at the urban background site in Paris in addition to traffic (Petit et al., 2014; Zhang et al., 2019). However, the relative importance of traffic and heating to HOA in different urban settings (e.g., kerbside and residential) and different seasons (e.g., heating and non-heating) remain
75 poorly understood.

In this study, the chemical composition of submicron aerosol (PM_{10}) at both kerbside and residential sites was simultaneously measured from 4 September to 9 November 2018 using an Aerodyne Aerosol Chemical Speciation (ACSM) and an Aethalometer. The chemical composition of PM_{10} and sources of OA at these two sites were explicitly characterized and compared during both the non-heating period and the heating period. Finally, the spatial variation and kerbside increment
80 of PM_{10} , as well as the implications for pollution mitigation strategies in Ireland were discussed.

2 Experimental

2.1 Sampling sites

Measurements were simultaneously conducted at a kerbside site in Dublin city centre and a residential site in sub-urban Dublin, at a distance of ~5 km from the kerbside site. The kerbside site is adjacent to a heavily trafficked street (i.e., Pearse Street)
85 with a traffic flow of ~46,000 vehicles per day, 76% of which consist of private cars, 13% of light goods vehicles, 7% of heavy goods vehicles, 2% of buses, and 2% of motorcycles (Fu et al., 2017). Pearse Street is characterised as an almost symmetrical street canyon i.e. rows of buildings on both sides of the road that are of equal height to the width of the street, and this affects local dispersion of air pollutants (Gallagher et al., 2013; Gallagher, 2016). It is worth noting that a bus stop was positioned ~20 m south from the sampling inlet. Measurements of submicron aerosol at the kerbside took place at ~ 3 m from the busy
90 street. The residential site is located on the campus of University College Dublin (UCD) in south Dublin. The nearest road is ~500 m away from the sampling site. Measurements at the site were conducted on the roof of the Science building (~30 m above the ground) at UCD from 4 September to 9 November 2018.

2.2 Instrumentation

95 A quadrupole Aerosol Chemical Speciation Monitor (q-ACSM, Aerodyne Research Inc.) and an aethalometer (AE-33, from Magee Scientific) were deployed at the kerbside site to measure the non-refractory PM_{10} (NR- PM_{10}) component (i.e. OA, sulfate, nitrate, ammonium, and chloride) and BC, respectively. At the residential site, another ACSM and aethalometer (AE-16) were



100 deployed to measure the PM_1 (NR- PM_1 and BC) composition simultaneously. At each site, ACSM and AE-33/16 were
sampling from the same $PM_{2.5}$ inlet line with isokinetic flow splitting. A detailed description of the ACSM and its operation is
given by Ng et al. (2011) and in our previous study (Lin et al., 2018). Briefly, an ACSM consists of a particle sampling inlet,
three vacuum chambers and a quadrupole mass spectrometer. During sampling, the ambient air was drawn into the cyclone
with a size cut-off of $2.5 \mu m$ at a flow rate of $3 L \text{ min}^{-1}$ to remove coarse particles. A Nafion dryer was used to dry the ambient
air before reaching the ACSM inlet. In the ACSM particle sampling inlet, the dried aerosol particles were focused into a narrow
105 aerosol beam through the aerodynamic lens system. The beam was directed onto a hot tungsten oven ($\sim 600 \text{ }^\circ\text{C}$) where the
particles were vaporized. The vaporized molecules were ionized by electron impact (70 eV) and the resulting ions were
analyzed by a quadrupole mass spectrometer. The time resolution of ACSM at the kerbside was set at 5 minutes to capture the
faster changing variation of PM composition adjacent to the busy road while a 1-hour interval was used at the residential site
to reduce uncertainty in measurement due to the relatively low concentrations. The ACSM standard data analysis software (v
1.6.1.0) in Igor 6.37 (WaveMetrics Inc.) was used to process the mass concentrations of NR- PM_1 components. To account for
110 the aerosol losses during sampling (Middlebrook et al., 2012), an composition dependent collection efficiency (CDCE) was
applied. The CDCE corrected NR- PM_1 shows a good agreement with the $PM_{2.5}$ measurement at another sub-urban site (Fig.
S1).

The AE-33 was deployed to measure black carbon (BC) at the kerbside with a time resolution of 1 minute while AE-16 at
the residential site had a time resolution of 5 minutes. AE-33 measures light absorption at seven wavelengths (370, 470, 520,
115 590, 660, 880, and 950 nm) (Drinovec et al., 2015) while AE-16 measures light absorption solely at 880 nm. BC mass
concentration was calculated from the change in optical attenuation at 880 nm in the selected time interval using the mass
absorption cross-section $7.77 \text{ m}^2 \text{ g}^{-1}$ (Drinovec et al., 2015).

Carbon monoxide analyzer (Thermo Scientific Model 48i) was employed to measure the CO mixing ratios with a time
resolution of 1 minute at the kerbside. NO-NO₂-NO_x analyzer (Thermo Scientific Model 42i) was employed to sample NO_x
120 with a time resolution of 1 minute at the kerbside and residential site simultaneously. Meteorological variables (temperature,
relative humidity, wind speed, and wind direction) with a time resolution of 1 hour were recorded at the meteorological stations
(Irish meteorological service) of Dublin airport (Fig. S2).

2.3 OA Source apportionment

125 Positive matrix factorization (PMF) with the multilinear engine (ME-2) was utilized for OA source apportionment by
constraining the reference profiles of certain factors. Because unconstrained PMF or free PMF often suffers from solution
ambiguity when some factors have similar temporal variation and/or factor profiles (Canonaco et al., 2013; Crippa et al., 2014;
Canonaco et al., 2015), the free PMF solution could potentially lead to solutions with mixed factors or inaccurate factor
attributions (Lanz et al., 2007; Canonaco et al., 2013). Thus, ME-2 was applied to get more environmentally meaningful
130 solutions by constraining the reference profiles with *a* value approach (Canonaco et al., 2013; Lin et al., 2017).



In this study, ME-2 was conducted on the interface of SoFi 6.8 (Canonaco et al., 2013). The reference profiles of peat, coal, and wood were taken from previous study by Lin et al. (2017) while the HOA and COA were obtained from a study in Paris by (Crippa et al., 2013). A sensitivity analysis was undertaken by varying the a values (0-0.5 or 0-50% variation) to evaluate the OA factor contribution at different levels of constraint on the reference factor (See the supplementary section of OA source
135 apportionment for the systematic selection of factors and evaluation of PMF solution ambiguity).

3 Results and discussion

Figure S1 shows the overview of the measurement at both the kerbside and the residential site from 4 September to 9 November 2018. The air quality during the early stage of the sampling period (before 30 September) showed limited influence from residential heating as observed by few pollution spikes in the evening when compared to a later period (From 1 October to 09
140 November; Fig. S1). Two periods, P1 from 10 to 17 September which represented the non-heating period and P2 from 27 October to 4 November represented the heating period, were selected as the focus of this study. The meteorological parameters including wind speed, wind direction, relative humidity (RH), and temperature during P1 and P2 are shown in Fig. S2. Specifically, during P1, south-westerly winds were prevailing, with an average wind speed of 4.5 m s^{-1} , ranging from 1.5 to 9.0 m s^{-1} while, during P2, the wind speeds were slightly lower with an average of 3.7 m s^{-1} (range 0.5 - 8.5 m s^{-1}). The low
145 wind speeds were accompanied by the northerly and easterly winds during P2. The temperature during P1 averaged $13.1 \text{ }^\circ\text{C}$, ranging from $8.6 \text{ }^\circ\text{C}$ to $18.2 \text{ }^\circ\text{C}$ while it was lower during P2 with an average of $4.5 \text{ }^\circ\text{C}$ (range -3.9 - $11.6 \text{ }^\circ\text{C}$). However, the RH during the P1 and P2 were similar, with an average RH of 78.7% (range 57 - 96%) for P1 and 78.9% (range 44 - 98%) for P2.

3.1 Mass concentration and chemical composition of PM_{10} during the P1 period

150 3.1.1 PM_{10} at the kerbside during P1

Figure 1 and Figure 2 show the time series and relative fractions of PM_{10} component (i.e., OA, sulfate, nitrate, ammonium, and chloride, and BC), respectively. At the kerbside, BC was the most dominant PM_{10} component, on average accounting for over half (55% or $5.6 \mu\text{g m}^{-3}$) of PM_{10} , followed by OA (32% or $3.3 \mu\text{g m}^{-3}$), sulfate (5% or $0.5 \mu\text{g m}^{-3}$), ammonium (4% or $0.4 \mu\text{g m}^{-3}$), nitrate (3% or $0.3 \mu\text{g m}^{-3}$), and chloride (1% or $0.1 \mu\text{g m}^{-3}$). In particular, frequent BC spikes ($> 15 \mu\text{g m}^{-3}$) affected
155 the local air quality substantially during the daytime ($6:00 - 21:00$, local time) and showed higher intensity during rush hours on weekdays. Similar patterns were also observed for NO_x (Fig. S3) and CO (Fig. S4) at the kerbside, confirming common traffic sources.

BC spikes were on the time scale of minutes, indicating certain types of vehicles were the major cause of such pollution plumes. The diesel-powered public buses were firstly suspected as the major emitters of BC because a bus stop was nearby,
160 about $\sim 20 \text{ m}$ away from the sampling site. Note the bus services usually start at $\sim 5:30$ and end at $\sim 23:00$ in downtown Dublin. However, BC spikes were also observed during other times e.g., from $23:00$ to $5:30$ when public bus services were not available.



Moreover, higher intensity and frequency of BC spikes were observed during the morning and evening rush hour peaks. Thus, in addition to the buses, other types of vehicles (e.g., private cars) were also potential contributors to the air pollution. Specifically, ~50 vehicles (manual count) were jammed along the nearby street during rush hours and higher emissions might be associated with the cold starts and idling speeds during such traffic jam. Additionally, the street canyon effect, making the pollutants hard to disperse, were also important factors in driving the high BC concentrations at the kerbside. In particular, the street canyon effect was evidenced by the high background BC concentration ($3.0 \mu\text{g m}^{-3}$) during the night (from 23:00 to 5:00) when traffic flow was at the lowest (Fig. 3a). As a comparison, the average BC was only $0.4 \mu\text{g m}^{-3}$ at the residential site during non-heating period (Table 1).

Similar to BC at the kerbside, OA also shows frequent spikes with concentrations of $>5 \mu\text{g m}^{-3}$ from 6:00 to 21:00 (Fig. 1a). However, in addition to traffic, cooking and secondary formation were also contributing to the OA mass at the kerbside (discussed in Sect. 3.3). In contrast to BC and OA, the time series of the measured inorganic aerosols were relatively smooth (Fig. 1), and did not exhibit any obvious influence from traffic. This is not surprising because vehicles are not direct emitters of these inorganic species, and the introduction of the threshold of 10 ppm (by mass) sulfur for gas/diesel oil led to very low sulphur emissions in Dublin (Regulations, 2008). On average, the sum of inorganic aerosol accounted for a relatively small fraction (13%) of the total PM_{10} (Fig. 2).

3.1.2 PM_{10} at the residential site during P1

The time series of OA, sulfate, nitrate, ammonium, and chloride at the residential site during P1 are shown in Fig. 1b. Over the entire P1 period, the average concentration of PM_{10} was $2.3 \mu\text{g m}^{-3}$ at the residential site, around five times lower than that at the kerbside. OA was the most dominant species at the residential site, accounting for 46% ($1.0 \mu\text{g m}^{-3}$) of PM_{10} (Fig. 2b), followed by BC (17% or $0.4 \mu\text{g m}^{-3}$), sulfate (17% or $0.4 \mu\text{g m}^{-3}$), ammonium (14% or $0.3 \mu\text{g m}^{-3}$), nitrate (5% or $0.1 \mu\text{g m}^{-3}$), and chloride (1% or $<0.1 \mu\text{g m}^{-3}$). Despite the fact that the measurements at the residential and kerbside were conducted simultaneously, all of the PM_{10} components showed no obvious trend that could be associated with vehicular emissions at the residential site (Fig. 3b), indicating the impact of traffic emissions from the kerbside had a minor impact on the residential site. Consistently, NO_x concentrations were very low with an average mixing ratio of NO_x of 2.6 ppb (median was 2.0 ppb; Table 1). The low impact of vehicular emissions on air quality at the residential site might be associated with the distance from the emission sources, as well as the effects of wind speed and wind direction. Specifically, the distance between the residential site and the nearest road is ~500 m and ~5 km away from the city centre. South-westerly wind was dominant during P1 with an average wind speed of 4.5 m s^{-1} , ranging from 1.5 to 9.0 m s^{-1} (Fig. S2).

190



3.2 Mass concentration and chemical composition of PM₁ during the P2 period

3.2.1 PM₁ at the kerbside during P2

During the heating period of P2, large pollution spikes were observed in the evening (20:00-23:00) with a simultaneous increase in all NR-PM₁ components and BC (Fig. 1c). Specifically, in the evening on 31 October, the peak PM₁ concentration was 197.3 $\mu\text{g m}^{-3}$ (Fig. 1c) which was more than four times higher than the rush hour peak on the same day. Moreover, the evening pollution expanded over the entire evening and went into the night, demonstrating the extensive impact from residential heating activities. On the same day, BC concentration increased up to 50 $\mu\text{g m}^{-3}$ in the evening, more than ten times higher than the average. The simultaneous increase in all NR-PM₁ components along with BC suggest common heating sources in the evening.

Over the entire period of P2, the average PM₁ concentration was 18.4 $\mu\text{g m}^{-3}$, around two times higher than that during P1 (Fig. 2c). While the average BC concentration increased from 5.6 $\mu\text{g m}^{-3}$ during P1 to 7.1 $\mu\text{g m}^{-3}$ during P2, the corresponding BC fraction decreased from 55% to 38%. This is due to the relatively high emissions of other PM₁ components (e.g., OA) which were associated with heating sources. Specifically, the average OA concentration was doubled during P2 (6.5 $\mu\text{g m}^{-3}$) than during P1 (3.3 $\mu\text{g m}^{-3}$) with the corresponding fraction increasing from 32% to 35%. Moreover, the average concentration and fraction of sulfate, nitrate, ammonium, and chloride also increased. On average, the fraction of inorganic components increased from 13% (1.3 $\mu\text{g m}^{-3}$) during P1 to 27% (6.1 $\mu\text{g m}^{-3}$) during P2. Among these inorganics, nitrate saw the largest increase from 3% (0.28 $\mu\text{g m}^{-3}$) during P1 to 9% (1.6 $\mu\text{g m}^{-3}$) during P2, partly due to the cold temperature (Fig. S2) which favoured the gas-to-particle partitioning of semi-volatile NH₄NO₃.

3.2.2 PM₁ at the residential site during P2

The time series of the measured PM₁ components at the residential during P2 is shown in Fig. 1d. During this period, the pollution spikes with a simultaneous increase in the concentrations of NR-PM₁ and BC were observed almost every evening. This was in great contrast to that during P1 when no clear pattern in NR-PM₁ species was observed. Moreover, the pollution spikes of NR-PM₁ at the residential site showed a simultaneous increase with that at the kerbside (Fig. 1c) and the PM_{2.5} at the Rathmines station (Fig. S1), indicating the three sites were affected by similar residential burning sources and air masses. Over the entire P2, the average PM₁ concentration was 12.7 $\mu\text{g m}^{-3}$, which was six times higher than during P1. On average, OA accounted for 63% (8.1 $\mu\text{g m}^{-3}$) of PM₁, making it the most dominant component (Fig. 2d), followed by BC (9% or 2.4 $\mu\text{g m}^{-3}$), nitrate (8% or 1.1 $\mu\text{g m}^{-3}$), ammonium (8% or 1.0 $\mu\text{g m}^{-3}$), sulfate (7% or 0.9 $\mu\text{g m}^{-3}$), and chloride (4% or 0.6 $\mu\text{g m}^{-3}$).



220 3.3 Sources of OA

3.3.1 OA factors at the kerbside

Figure 4 and Figure 5 show the fractional contributions and diurnal cycles of the resolved OA factors, respectively. Three OA factors were resolved during P1 at the kerbside, including traffic-related HOA, cooking OA (COA), and oxygenated OA (OOA). Despite being adjacent to the busy road in Dublin city centre, HOA accounted for only 27% ($0.9 \mu\text{g m}^{-3}$) of the total
225 OA (Fig. 4a) with rest attributing to COA (36% or $1.2 \mu\text{g m}^{-3}$) and OOA (37% or $1.2 \mu\text{g m}^{-3}$). The diurnal cycle of HOA featured two rush hour peaks which were consistent with that of BC, confirming its traffic source (Fig. 5a). Specifically, the HOA concentration was very low ($0.1 \mu\text{g m}^{-3}$) from 00:00 to 5:00, indicating a low background HOA concentration. From 6:00, the HOA concentration increased to a peak value of $1.5 \mu\text{g m}^{-3}$ at 8:00. After the morning rush hour peak, the HOA concentration was constantly high ($1 \mu\text{g m}^{-3}$) and reached to $1.3 \mu\text{g m}^{-3}$ at the evening rush hour peak (17:00). The HOA
230 returned to the background level at 23:00, corresponding to reduced traffic emissions during the night (Fu et al., 2017).

The high contribution (36%) of COA was associated with location the sampling site in Dublin city centre with some restaurants around. The diurnal pattern of COA showed a lunch time peak at 13:00 and dinner time peak at 20:00, corresponding to the meal times. Higher dinner time COA peak ($2.7 \mu\text{g m}^{-3}$) was observed than lunch time peak ($1.6 \mu\text{g m}^{-3}$) likely due to higher emissions during the evening coupled with relatively low evening temperatures (Fig. S2).

235 The OOA profile (Fig. S7) resembled the less volatile OOA (LV-OOA) which usually represents well-aged SOA (Canonaco et al., 2013; Crippa et al., 2014). However, the diurnal pattern of OOA in Dublin showed a clear pattern that was strongly influenced by local sources and was most likely from fresh SOA instead of well-aged SOA. Moreover, the morning peak of OOA came about 1 hour later than that for HOA, probably indicating fast SOA formation processes by atmospheric oxidation of SOA precursor gases and/or condensation of semi-volatile VOCs emitted by the nearby traffic. In addition, the
240 contribution from cooking sources to OOA was also important as evidenced by the concurrent peaks of OOA with COA. The OOA had a background concentration of $0.5 \mu\text{g m}^{-3}$ which was higher than HOA ($0.1 \mu\text{g m}^{-3}$) and COA ($0.1 \mu\text{g m}^{-3}$), indicating part of OOA was also associated with regional transport.

During P2, solid fuel burning related OA factors, including wood, peat, and coal, were resolved in addition to HOA, COA, and OOA (Fig. 4c and 5c). Consistent with that for P1, the HOA factor also showed rush hour peaks in the morning (\sim 8:00) and afternoon (\sim 17:00) with similar concentrations (\sim $1.5 \mu\text{g m}^{-3}$) during P2 to that during P1. However, a third HOA peak was
245 also seen at \sim 22:00 (Fig. 5c), indicating additional sources from residential heating likely from oil burning (CSO, 2016; Lin et al., 2017; Lin et al., 2018). Over the entire P2, HOA accounted for 18% ($1.2 \mu\text{g m}^{-3}$) of OA (Fig. 4c). The relatively small fraction of HOA, again, indicates traffic was not the dominant OA sources despite being adjacent to the busy road in downtown Dublin. Note that HOA during P2 could only be taken as upper limit of the primary OA emissions from traffic because the
250 additional contribution from the oil burning.

COA showed a similar diurnal pattern to that during P1 but with slightly higher concentrations during P2, which could be associated with colder temperature and shallower boundary layer. On average, COA accounted for 18% ($1.2 \mu\text{g m}^{-3}$) of OA



(Fig. 4c). Solid fuel burning accounted for 33% ($2.1 \mu\text{g m}^{-3}$) of the total OA. Moreover, higher OOA concentrations were observed in the evening and night, indicating an important contribution from the condensation of SVOCs emitted from solid fuel burning.

3.3.2 OA factors at the residential site

During P1, OOA, HOA, and peat factors were resolved at the residential site (Fig. 4b and 5b). OOA accounted for the majority (65% or $0.6 \mu\text{g m}^{-3}$) of OA. HOA accounted for a low fraction (15% or $0.1 \mu\text{g m}^{-3}$) of OA while peat accounted for 20% ($0.2 \mu\text{g m}^{-3}$) of OA. The absolute concentration of HOA at the residential site was approximately ten times lower (0.1 vs $1.0 \mu\text{g m}^{-3}$) than that at the kerbside. The low contribution of HOA at the residential site was expected because HOA, on average, contributed to only 27% of OA even adjacent to the busy road in Dublin city centre (Fig. 4a). The low contribution of HOA is also consistent with the low mixing ratio of NO_x at the residential site (median: 2.0 ppb) which was ~ 20 times lower than that at the kerbside (Table 1).

During P2, the OA factors, including OOA, wood, peat, coal and HOA, all showed peak concentrations during the night (Fig. 5b). In contrast, during the day, all factors showed very low concentrations ($<0.5 \mu\text{g m}^{-3}$) despite the high spikes in the evening. HOA at the residential site was attributed to the oil burning because no rush hour peaks of traffic-related HOA were observed at this site. HOA, on average, accounted for 18% ($1.6 \mu\text{g m}^{-3}$) of OA. Solid fuel burning OA factors showed the largest enhancement with the sum of peat, coal, and wood factors accounting for 50% ($4.3 \mu\text{g m}^{-3}$) of OA. OOA, on average, accounted for 32% ($2.8 \mu\text{g m}^{-3}$) of OA and the higher OOA concentration during the evening again suggested its major source was from the condensation of SVOCs emitted from solid fuel burning.

3.4 Kerbside increment of PM_{10}

Figure 6 shows the comparison of the measured PM_{10} components and NO_x between the kerbside and residential site during P1 and P2. Among the measured PM_{10} species, BC showed the largest kerbside increment, with an increment ratio of 16 (median value) during the P1 period (Fig. 6). During the P2 period, BC increment ratio was slightly lower (10) primarily due to the additional emission sources of solid fuel burning affecting both sites simultaneously. BC showed peak concentration during rush hour peaks, corresponding to heavier traffic during these times (Fig. 3). As expected, the kerbside increment of BC was more enhanced during rush hour peaks (Fig. S16), reaching up to 25 for BC. When traffic emissions were at their lowest at night, a small but significant BC increment of 5 was observed, partially due to the street canyon effects, creating a poor dispersion condition in the downtown areas. The kerbside increment of BC was primarily due to vehicular emissions and this was corroborated by the gas pollutant of NO_x which showed an increment ratio of 7-23 (Fig. 6). Note that our measurement represents the average fleet in Dublin and thus the high kerbside increment for BC in Dublin have significant implications for



the potentially higher exposure risk at the kerbside. For example, Ljungman et al. (2019) associated higher risk of stroke for exposure to ambient BC from traffic exhaust.

Compared to BC, the kerbside increment of OA was less significant because traffic was not a major source of OA. However, higher OA increment ratio (3; median value) was also seen during P1 than during P2 (1.5) due to the combined contributions from sources like traffic, cooking, solid fuel burning and secondary formation (see Sect. 3.3). As a comparison, the concentrations of sulfate, nitrate, and ammonium did not show large variations between the two sites again because vehicles are not direct emitters of these secondary aerosols. Instead, the good correlation ($R^2=0.53-0.85$ and slopes= $0.70-0.83$; Fig. S17) for the time series of these inorganic aerosols between the two sites, suggesting common sources from e.g., regional transport.

3.5 Implications for emission control

The HOA/BC ratio was ~ 0.16 as achieved from the slope of the linear regression between HOA and BC with a R^2 of 0.6 (Fig. S18), indicating the average traffic in Dublin emitted approximately six times more BC than HOA. Compared to other studies, the HOA/BC ratio in Dublin was lower than the HOA/BC ratios reported for gasoline vehicles-dominated environment but was similar to the diesel environment (0.26) adjacent to the highway in Grenoble (DeWitt et al., 2015), indicating most of the traffic emissions were from diesel vehicles. Actually, diesel fuel accounted for 73% of the on-road transport energy in Ireland in 2017 (Fig. 7a). Figure 7 also shows an increasing trend of diesel fuel usage, indicating worse air quality in the predictable future at the kerbside if diesel vehicular emissions were not controlled.

This study also shows that vehicular emissions appear to impact the air quality adjacent to the roads. In contrast, solid fuel burning has a large geographic impact, affecting overall air quality at the kerbside and residential sites examined in this investigation. Such large geographic impact suggests significant climate effects from residential emissions (Butt et al., 2016) which contain a higher fraction of OA than that for traffic. However, surprisingly, the governmental census data shows only a few households ($<5\%$) consumed these solid fuels with the majority households ($\sim 95\%$) used natural gas and electricity as the primary heating sources in 2016 (Fig. 7b). Therefore, if the emissions from this small fraction of households were controlled, good overall air quality and less climate forcing can be expected.

4 Conclusion

The chemical composition and sources of submicron aerosol (PM_{10}) were simultaneously investigated at a kerbside location in downtown Dublin and at a residential site in south Dublin (~ 5 km apart) using an ACSM and AE33/16 at both sites during both non-heating (i.e., early September) and heating periods (i.e., late October) of 2018. Traffic emissions were found to have a minor impact on air quality at the residential site due to the distance from nearby roadways and other affecting parameters such as wind speed and wind direction. In contrast, the kerbside was found to be highly affected by the diesel vehicular emissions. BC was the most dominant component (44-59%) of PM_{10} at the kerbside location while OA was the most important



315 species (43-61% of PM_{10}) at the residential site. During non-heating period, an increment ratio of up to 25 was found for the
BC at the kerbside when compared to the level of BC at the residential site primarily due to vehicular emissions. During the
heating period, the BC increment ratio was lower (~ 10) due to the additional sources of solid fuel burning which contributed
to the BC concentrations at both sites. Moreover, solid fuel burning was shown to increase PM_{10} concentrations substantially
with episodic concentrations of $>100 \mu g m^{-3}$ being recorded at both sites simultaneously. Source apportionment of OA using
320 ME-2 showed that only 18-27% of OA could be directly associated with vehicular emissions (i.e., HOA) at the kerbside, with
the larger contribution of OA being attributed to cooking, solid fuel burning, and OOA. HOA contributed to 15-18% of OA at
the residential site which was attributed to oil burning instead of traffic because HOA did not show rush hour peaks as found
at the residential site. During the heating period, solid fuel burning contributed to approximately 50% of OA at the residential
site, while oxygenated OA accounted for almost 65% of OA during the non-heating period. This study highlights the significant
325 increment of BC due to the traffic emissions at the kerbside and the large geographic impact of OA from residential heating at
both the kerbside and residential sites. Therefore, traffic and residential heating might have different health and climate
implications as suggested by the temporal and spatial variability of sources within Dublin city centre.

5 Data Availability

All data needed to evaluate the conclusions in the paper are present in the paper and/or the Supplementary Materials. Also, all
330 data used in the study are available from the corresponding author upon request.

6 Author Contribution

JO, DC, JW, and CO'D conceived and designed the experiments; CL, JO, DC, and PB performed the experiments; CL, JO,
WX, PB, JW, JG, RJH, and CO'D analyzed the data; CL prepared the manuscript with input from all co-authors.

7 Competing interests

335 The authors declare that they have no conflict of interest.

8 Acknowledgments

This work was supported by EPA-Ireland (AEROSOURCE, 2016-CCRP-MS-31), Department of Communications, Climate
Action and Environment (DCCA), the National Natural Science Foundation of China (NSFC) under grant no. 41925015,
91644219 and 41877408. The authors would also like to acknowledge the contribution of the COST Action CA16109
340 (COLOSSAL) and MaREI, the SFI Research Centre for Energy, Climate and Marine.



9 References:

- 345 An, Z., Huang, R.-J., Zhang, R., Tie, X., Li, G., Cao, J., Zhou, W., Shi, Z., Han, Y., Gu, Z., and Ji, Y.: Severe haze in northern China: A synergy of anthropogenic emissions and atmospheric processes, *Proc. Natl. Acad. Sci.*, 116, 8657-8666, 10.1073/pnas.1900125116, 2019.
- 350 Burnett, R., Chen, H., Szyszkowicz, M., Fann, N., Hubbell, B., Pope, C. A., Apte, J. S., Brauer, M., Cohen, A., Weichenthal, S., Coggins, J., Di, Q., Brunekreef, B., Frostad, J., Lim, S. S., Kan, H., Walker, K. D., Thurston, G. D., Hayes, R. B., Lim, C. C., Turner, M. C., Jerrett, M., Krewski, D., Gapstur, S. M., Diver, W. R., Ostro, B., Goldberg, D., Crouse, D. L., Martin, R. V., Peters, P., Pinault, L., Tjepkema, M., van Donkelaar, A., Villeneuve, P. J., Miller, A. B., Yin, P., Zhou, M., Wang, L., Janssen, N. A. H., Marra, M., Atkinson, R. W., Tsang, H., Quoc Thach, T., Cannon, J. B., Allen, R. T., Hart, J. E., Laden, F., Cesaroni, G., Forastiere, F., Weinmayr, G., Jaensch, A., Nagel, G., Concin, H., and Spadaro, J. V.: Global estimates of mortality associated with long-term exposure to outdoor fine particulate matter, *Proc. Natl. Acad. Sci.*, 115, 9592-9597, 10.1073/pnas.1803222115, 2018.
- 355 Butt, E. W., Rap, A., Schmidt, A., Scott, C. E., Pringle, K. J., Reddington, C. L., Richards, N. A. D., Woodhouse, M. T., Ramirez-Villegas, J., Yang, H., Vakkari, V., Stone, E. A., Rupakheti, M., S. Praveen, P., G. van Zyl, P., P. Beukes, J., Josipovic, M., Mitchell, E. J. S., Sallu, S. M., Forster, P. M., and Spracklen, D. V.: The impact of residential combustion emissions on atmospheric aerosol, human health, and climate, *Atmos. Chem. Phys.*, 16, 873-905, 10.5194/acp-16-873-2016, 2016.
- 360 Canonaco, F., Crippa, M., Slowik, J. G., Baltensperger, U., and Prévôt, A. S. H.: SoFi, an IGOR-based interface for the efficient use of the generalized multilinear engine (ME-2) for the source apportionment: ME-2 application to aerosol mass spectrometer data, *Atmos. Meas. Tech.*, 6, 3649-3661, 2013.
- Canonaco, F., Slowik, J. G., Baltensperger, U., and Prévôt, A. S. H.: Seasonal differences in oxygenated organic aerosol composition: Implications for emissions sources and factor analysis, *Atmos. Chem. Phys.*, 15, 6993-7002, 10.5194/acp-15-6993-2015, 2015.
- 365 Cohen, A. J., Brauer, M., Burnett, R., Anderson, H. R., Frostad, J., Estep, K., Balakrishnan, K., Brunekreef, B., Dandona, L., Dandona, R., Feigin, V., Freedman, G., Hubbell, B., Jobling, A., Kan, H., Knibbs, L., Liu, Y., Martin, R., Morawska, L., Pope, C. A., Shin, H., Straif, K., Shaddick, G., Thomas, M., van Dingenen, R., van Donkelaar, A., Vos, T., Murray, C. J. L., and Forouzanfar, M. H.: Estimates and 25-year trends of the global burden of disease attributable to ambient air pollution: an analysis of data from the Global Burden of Diseases Study 2015, *The Lancet*, 389, 1907-1918, [https://doi.org/10.1016/S0140-6736\(17\)30505-6](https://doi.org/10.1016/S0140-6736(17)30505-6), 2017.
- 370 Crippa, M., Decarlo, P. F., Slowik, J. G., Mohr, C., Heringa, M. F., Chirico, R., Poulain, L., Freutel, F., Sciare, J., Cozic, J., Di Marco, C. F., Elsasser, M., Nicolas, J. B., Marchand, N., Abidi, E., Wiedensohler, A., Drewnick, F., Schneider, J., Borrmann, S., Nemitz, E., Zimmermann, R., Jaffrezo, J. L., Prévôt, A. S. H., and Baltensperger, U.: Wintertime aerosol chemical composition and source apportionment of the organic fraction in the metropolitan area of Paris, *Atmos. Chem. Phys.*, 13, 961-981, 2013.
- 375 Crippa, M., Canonaco, F., Lanz, V. A., Äijälä, M., Allan, J. D., Carbone, S., Capes, G., Ceburnis, D., Dall'Osto, M., Day, D. A., DeCarlo, P. F., Ehn, M., Eriksson, A., Freney, E., Hildebrandt Ruiz, L., Hillamo, R., Jimenez, J. L., Junninen, H., Kiendler-Scharr, A., Kortelainen, A. M., Kulmala, M., Laaksonen, A., Mensah, A. A., Mohr, C., Nemitz, E., O'Dowd, C., Ovadnevaite, J., Pandis, S. N., Petäjä, T., Poulain, L., Saarikoski, S., Sellegri, K., Swietlicki, E., Tiitta, P., Worsnop, D. R., Baltensperger, U., and Prévôt, A. S. H.: Organic aerosol components derived from 25 AMS data sets across Europe using a consistent ME-2 based source apportionment approach, *Atmos. Chem. Phys.*, 14, 6159-6176, 10.5194/acp-14-6159-2014, 2014.
- 380 CSO: (Central Statistics Office). Private Households in Permanent Housing Units. <https://www.cso.ie/px/pxeirestat/Statire/SelectVarVal/Define.asp?maintable=E4015&PLanguage=0>, 2016.
- 385 DeWitt, H. L., Hellebust, S., Temime-Roussel, B., Ravier, S., Polo, L., Jacob, V., Buisson, C., Charron, A., André, M., Pasquier, A., Besombes, J. L., Jaffrezo, J. L., Wortham, H., and Marchand, N.: Near-highway aerosol and gas-phase measurements in a high-diesel environment, *Atmos. Chem. Phys.*, 15, 4373-4387, 2015.
- Drinovec, L., Močnik, G., Zotter, P., Prévôt, A. S. H., Ruckstuhl, C., Coz, E., Rupakheti, M., Sciare, J., Müller, T., Wiedensohler, A., and Hansen, A. D. A.: The "dual-spot" Aethalometer: an improved measurement of aerosol black carbon with real-time loading compensation, *Atmos. Meas. Tech.*, 8, 1965-1979, 2015.
- 390 Fu, M., Kelly, J. A., and Clinch, J. P.: Estimating annual average daily traffic and transport emissions for a national road network: A bottom-up methodology for both nationally-aggregated and spatially-disaggregated results, *J. Transp. Geogr.*, 58,



- 186-195, <https://doi.org/10.1016/j.jtrangeo.2016.12.002>, 2017.
- Fuzzi, S., Baltensperger, U., Carslaw, K., Decesari, S., Denier Van Der Gon, H., Facchini, M., Fowler, D., Koren, I., Langford, B., and Lohmann, U.: Particulate matter, air quality and climate: lessons learned and future needs, *Atmos. Chem. Phys.*, 15, 8217-8299, 2015.
- 395 Gallagher, J., Gill, L. W., and McNabola, A.: The passive control of air pollution exposure in Dublin, Ireland: A combined measurement and modelling case study, *Sci. Total Environ.*, 458-460, 331-343, <https://doi.org/10.1016/j.scitotenv.2013.03.079>, 2013.
- Gallagher, J.: A modelling exercise to examine variations of NO_x concentrations on adjacent footpaths in a street canyon: The importance of accounting for wind conditions and fleet composition, *Sci. Total Environ.*, 550, 1065-1074, <https://doi.org/10.1016/j.scitotenv.2016.01.096>, 2016.
- 400 Gentner, D. R., Jathar, S. H., Gordon, T. D., Bahreini, R., Day, D. A., El Haddad, I., Hayes, P. L., Pieber, S. M., Platt, S. M., de Gouw, J., Goldstein, A. H., Harley, R. A., Jimenez, J. L., Prévôt, A. S. H., and Robinson, A. L.: Review of Urban Secondary Organic Aerosol Formation from Gasoline and Diesel Motor Vehicle Emissions, *Environ. Sci. Technol.*, 51, 1074-1093, 10.1021/acs.est.6b04509, 2017.
- 405 Hallquist, M., Wenger, J. C., Baltensperger, U., Rudich, Y., Simpson, D., Claeys, M., Dommen, J., Donahue, N. M., George, C., Goldstein, A. H., Hamilton, J. F., Herrmann, H., Hoffmann, T., Iinuma, Y., Jang, M., Jenkin, M. E., Jimenez, J. L., Kiendler-Scharr, A., Maenhaut, W., McFiggans, G., Mentel, T. F., Monod, A., Prévôt, A. S. H., Seinfeld, J. H., Surratt, J. D., Szmigielski, R., and Wildt, J.: The formation, properties and impact of secondary organic aerosol: current and emerging issues, *Atmos. Chem. Phys.*, 9, 5155-5236, 2009.
- 410 Lanz, V. A., Alfarra, M. R., Baltensperger, U., Buchmann, B., Hueglin, C., and Prévôt, A. S. H.: Source apportionment of submicron organic aerosols at an urban site by factor analytical modelling of aerosol mass spectra, *Atmos. Chem. Phys.*, 7, 1503-1522, 10.5194/acp-7-1503-2007, 2007.
- Lenschow, P., Abraham, H. J., Kutzner, K., Lutz, M., Preuß, J. D., and Reichenbacher, W.: Some ideas about the sources of PM₁₀, *Atmos. Environ.*, 35, S23-S33, [https://doi.org/10.1016/S1352-2310\(01\)00122-4](https://doi.org/10.1016/S1352-2310(01)00122-4), 2001.
- 415 Lin, C., Ceburnis, D., Hellebust, S., Buckley, P., Wenger, J., Canonaco, F., Prévôt, A. S. H., Huang, R.-J., O'Dowd, C., and Ovadnevaite, J.: Characterization of primary organic aerosol from domestic wood, peat, and coal burning in Ireland, *Environ. Sci. Technol.*, 51, 10624-10632, 2017.
- Lin, C., Huang, R.-J., Ceburnis, D., Buckley, P., Preissler, J., Wenger, J., Rinaldi, M., Facchini, M. C., O'Dowd, C., and Ovadnevaite, J.: Extreme air pollution from residential solid fuel burning, *Nat. Sustain.*, 1, 512-517, 2018.
- 420 Lin, C., Ceburnis, D., Huang, R.-J., Canonaco, F., Prévôt, A. S. H., O'Dowd, C., and Ovadnevaite, J.: Summertime Aerosol over the West of Ireland Dominated by Secondary Aerosol during Long-Range Transport, *Atmos.*, 10, 59-70, <https://doi.org/10.3390/atmos10020059>, 2019a.
- Lin, C., Ceburnis, D., Huang, R. J., Xu, W., Spohn, T., Martin, D., Buckley, P., Wenger, J., Hellebust, S., Rinaldi, M., Facchini, M. C., O'Dowd, C., and Ovadnevaite, J.: Wintertime aerosol dominated by solid-fuel-burning emissions across Ireland: insight into the spatial and chemical variation in submicron aerosol, *Atmos. Chem. Phys.*, 19, 14091-14106, 10.5194/acp-19-14091-2019, 2019b.
- 425 Ljungman, P. L., Andersson, N., Stockfelt, L., Andersson, E. M., Nilsson Sommar, J., Eneroth, K., Gidhagen, L., Johansson, C., Lager, A., and Leander, K.: Long-Term Exposure to Particulate Air Pollution, Black Carbon, and Their Source Components in Relation to Ischemic Heart Disease and Stroke, *Environ. Health Persp.*, 127, 107012, 2019.
- 430 Middlebrook, A. M., Bahreini, R., Jimenez, J. L., and Canagaratna, M. R.: Evaluation of Composition-Dependent Collection Efficiencies for the Aerodyne Aerosol Mass Spectrometer using Field Data, *Aerosol Sci. Tech.*, 46, 258-271, 10.1080/02786826.2011.620041, 2012.
- Mohr, C., Richter, R., DeCarlo, P. F., Prévôt, A. S. H., and Baltensperger, U.: Spatial variation of chemical composition and sources of submicron aerosol in Zurich during wintertime using mobile aerosol mass spectrometer data, *Atmos. Chem. Phys.*, 11, 7465-7482, 10.5194/acp-11-7465-2011, 2011.
- 435 Mues, A., Manders, A., Schaap, M., van Ulft, L. H., van Meijgaard, E., and Builtjes, P.: Differences in particulate matter concentrations between urban and rural regions under current and changing climate conditions, *Atmos. Environ.*, 80, 232-247, <https://doi.org/10.1016/j.atmosenv.2013.07.049>, 2013.
- 440 Ng, N. L., Herndon, S. C., Trimborn, A., Canagaratna, M. R., Croteau, P. L., Onasch, T. B., Sueper, D., Worsnop, D. R., Zhang, Q., Sun, Y. L., and Jayne, J. T.: An Aerosol Chemical Speciation Monitor (ACSM) for routine monitoring of the composition



- and mass concentrations of ambient aerosol, *Aerosol Sci. Technol.*, 45, 780-794, 2011.
- Petit, J. E., Favez, O., Sciare, J., Canonaco, F., Croteau, P., Močnik, G., Jayne, J., Worsnop, D., and Leoz-Garziandia, E.: Submicron aerosol source apportionment of wintertime pollution in Paris, France by double positive matrix factorization (PMF2) using an aerosol chemical speciation monitor (ACSM) and a multi-wavelength Aethalometer, *Atmos. Chem. Phys.*, 14, 13773-13787, 10.5194/acp-14-13773-2014, 2014.
- 445 Pope III, C. A., Burnett, R. T., Thun, M. J., Calle, E. E., Krewski, D., Ito, K., and Thurston, G. D.: Lung cancer, cardiopulmonary mortality, and long-term exposure to fine particulate air pollution, *Jama*, 287, 1132-1141, 2002.
- Regulations: Sulphur Content of Heavy Fuel Oil, Gas Oil, and Marine Fuels Regulations, 2008.
- Zhang, R., Wang, G., Guo, S., Zamora, M. L., Ying, Q., Lin, Y., Wang, W., Hu, M., and Wang, Y.: Formation of Urban Fine Particulate Matter, *Chem. Rev.*, 115, 3803-3855, 10.1021/acs.chemrev.5b00067, 2015.
- 450 Zhang, Y., Favez, O., Petit, J. E., Canonaco, F., Truong, F., Bonnaire, N., Cretnn, V., Amodeo, T., Prévôt, A. S. H., Sciare, J., Gros, V., and Albinet, A.: Six-year source apportionment of submicron organic aerosols from near-continuous highly time-resolved measurements at SIRTa (Paris area, France), *Atmos. Chem. Phys.*, 19, 14755-14776, 10.5194/acp-19-14755-2019, 2019.
- 455



Table 1: Mean, standard deviation (SD), first quartile (Q1), median, third quartile (Q3), and maximum (Max) concentration of organic aerosol (OA), sulfate (SO₄), nitrate (NO₃), ammonium (NH₄), chloride (Chl), and black carbon (BC) at the kerbside and residential site during period P1 (see Fig. S1 for definition of P1). All are in $\mu\text{g m}^{-3}$.

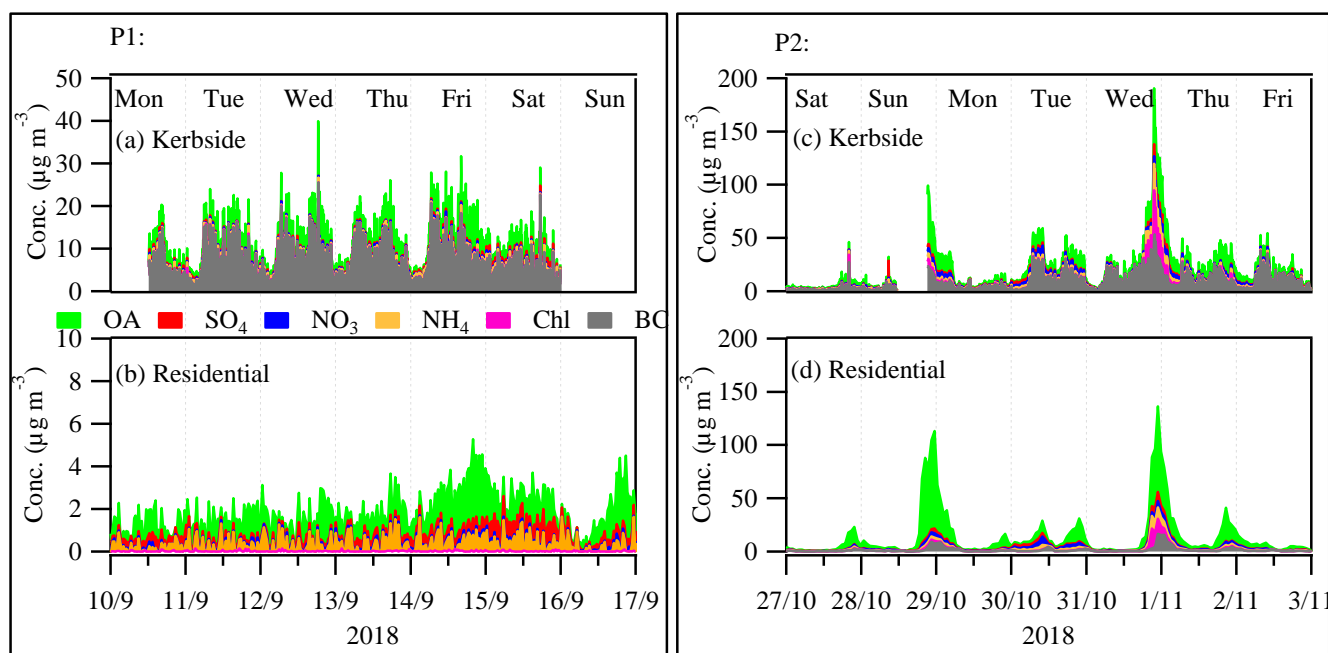
	Kerbside						Residential					
	mean	SD	Q1	median	Q3	Max	mean	SD	Q1	median	Q3	Max
OA	3.33	2.09	1.79	3.01	4.30	22.73	1.04	0.75	0.48	0.93	1.43	3.93
SO ₄	0.52	0.38	0.24	0.44	0.68	2.7	0.38	0.21	0.23	0.33	0.47	1.23
NO ₃	0.28	0.16	0.16	0.24	0.34	1.38	0.11	0.06	0.06	0.09	0.14	0.35
NH ₄	0.42	0.46	0	0.3	0.66	3.86	0.32	0.38	0.00	0.23	0.50	1.64
Chl	0.1	0.26	0.02	0.06	0.12	4.98	0.02	0.03	0.00	0.00	0.03	0.15
BC ^a	5.63	4.58	2.64	4.58	7.34	67.00	0.39	0.39	0.18	0.28	0.43	2.99
NO _x	54.14	42.68	17.40	45.10	79.85	272.10	2.63	2.28	0.80	2.00	3.95	12.90

460 ^aBC at the residential site was not available during P1 and the week after (from 24 September to 30 September) was shown as a reference of the BC concentration during non-heating period.

Table 2. Mean, standard deviation (SD), first quartile (Q1), median, third quartile (Q3), and maximum (Max) concentration of organic aerosol (OA), sulfate (SO₄), nitrate (NO₃), ammonium (NH₄), chloride (Chl), and black carbon (BC) at the kerbside and residential site during period P2 (see Fig. S1 for definition of P2). All are in $\mu\text{g m}^{-3}$.

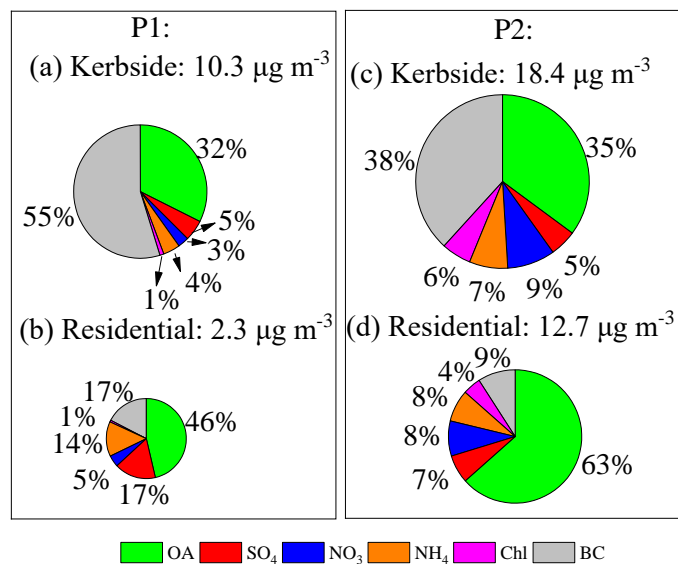
	Kerbside						Residential					
	mean	SD	Q1	median	Q3	Max	mean	SD	Q1	median	Q3	Max
OA	6.47	7.91	1.42	3.71	8.30	53.2	8.07	15.53	0.90	2.33	6.95	91.79
SO ₄	0.92	1.38	0.2	0.46	1.06	15.9	0.87	1.26	0.21	0.41	1.01	8.54
NO ₃	1.64	1.92	0.2	0.72	2.62	9.68	1.08	1.43	0.12	0.42	1.53	7.95
NH ₄	1.32	2.5	0.1	0.66	1.52	26.1	0.99	1.65	0.17	0.53	1.25	11.88
Chl	1.02	3.86	0.04	0.14	0.38	47.7	0.56	2.12	0.02	0.06	0.23	18.66
BC	7.05	8.27	1.41	3.76	9.64	53.4	1.16	2.38	0.17	0.38	0.98	23.31
NO _x	89.71	85.54	28.50	60.30	123.45	478.10	16.49	22.55	3.60	8.20	18.00	162.80

465



470

Figure 1. Time series of submicron organic aerosol (OA), sulfate (SO_4), nitrate (NO_3), ammonium (NH_4), chloride (Chl), and black carbon (BC) during P1 (left panel) and P2 (right panel) at the kerbside (a, c) and residential (b, d) (see Fig. S1 for the selection of P1 and P2). Note that the time resolution for the ACSM at the kerbside was 5 min while it was 1 h at the residential site, and BC data were averaged to match the time step of ACSM. Also shown are the day of the week, including Monday (Mon), Tuesday (Tue), Wednesday (Wed), Thursday (Thu), Friday (Fri), Saturday (Sat), and Sunday (Sun).



475

Figure 2. Relative contribution of submicron organic aerosol (OA), sulfate (SO₄), nitrate (NO₃), ammonium (NH₄), chloride (Chl) and black carbon (BC) during P1 and P2 at the kerbside (a, c) and residential (b, d). The values above the pie charts are the mean concentration of PM₁ for each site during P1 or P2 and the area of the pie was proportional to the mean concentration.



480

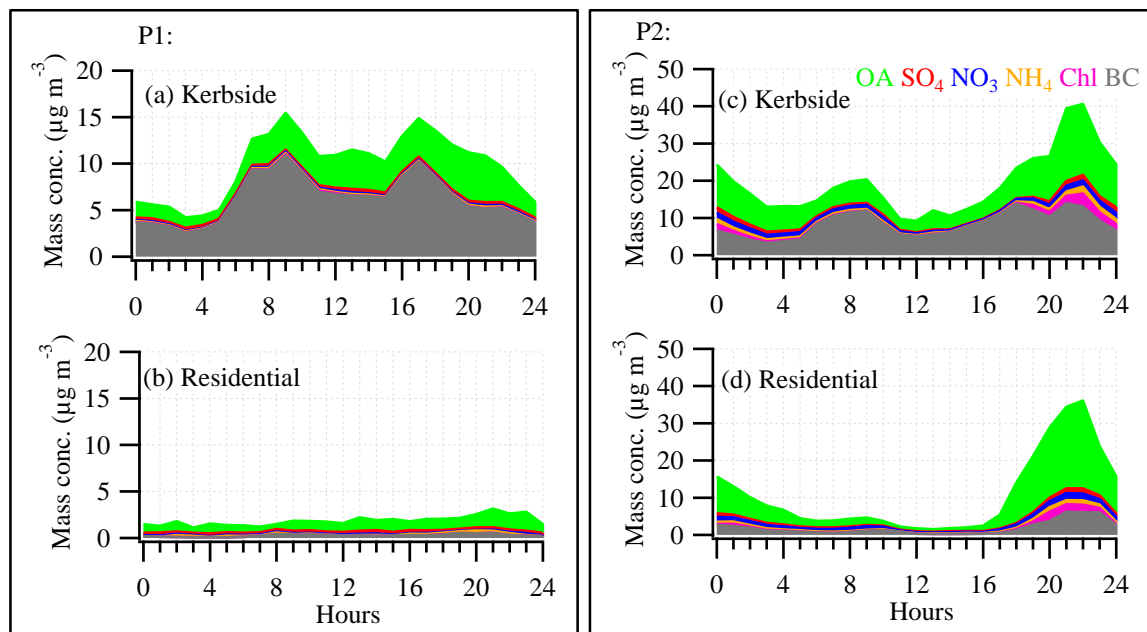


Figure 3. The diurnal cycle of submicron organic aerosol (OA), sulfate (SO_4), nitrate (NO_3), ammonium (NH_4), chloride (Chl), and black carbon (BC) during P1 (left panel) and P2 (right panel) at the kerbside (a, c) and residential site (b, d).

485

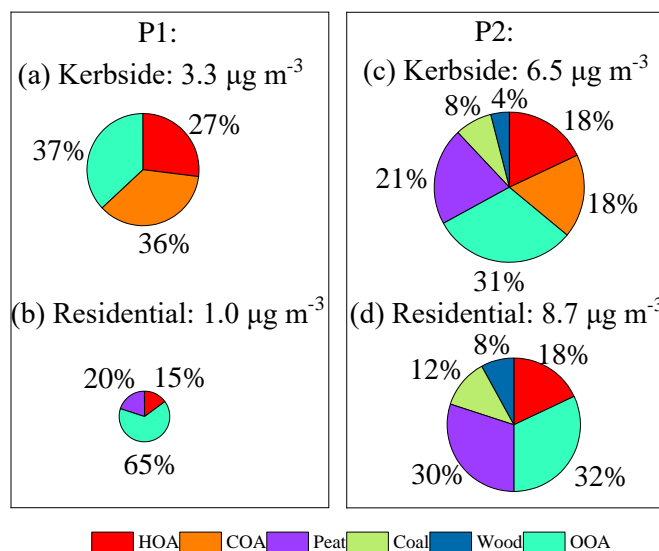
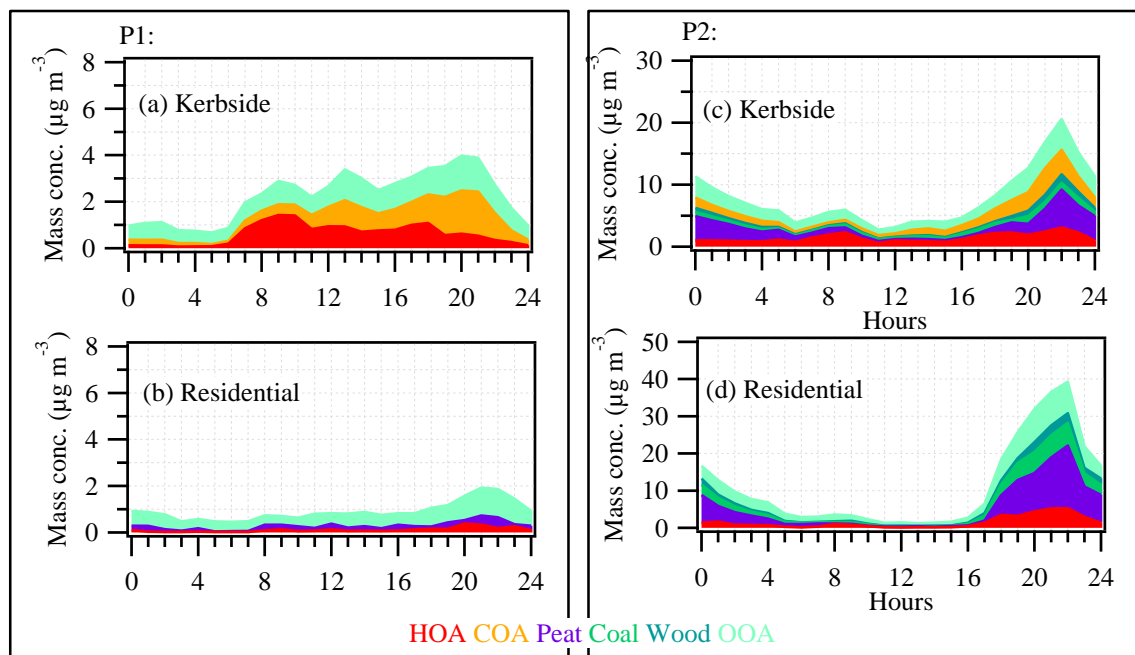
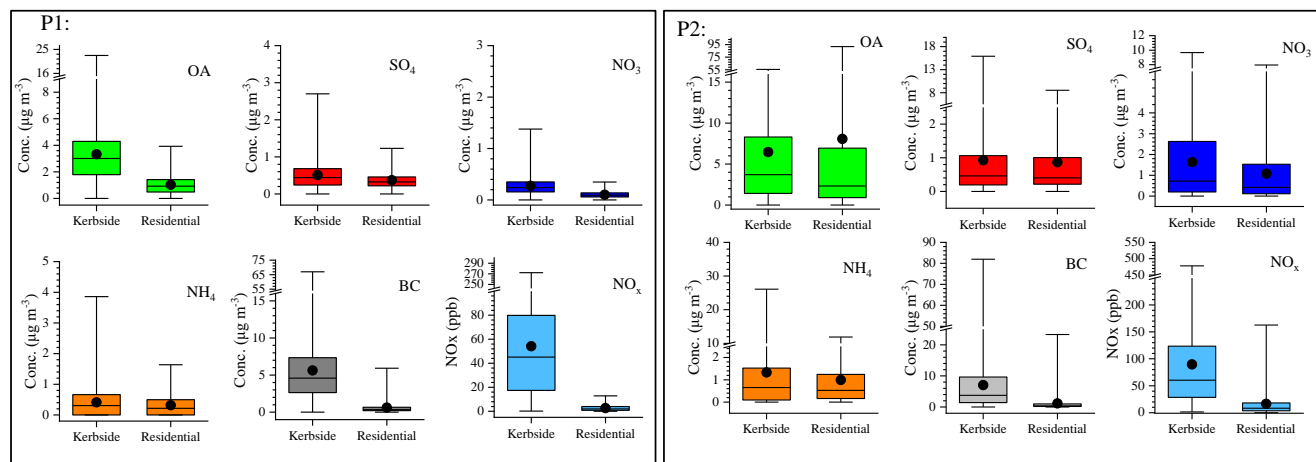


Figure 4. Relative contribution of organic aerosol (OA) factors, including Hydrocarbon-like OA (HOA), cooking (COA), peat, coal, wood, and oxygenated OA (OOA) during P1 and P2 at the kerbside (a, c) and residential site (b, d). The values above the pie charts are the mean concentration of OA for the site during P1 or P2 and the area of the pie was proportional to the mean concentration.



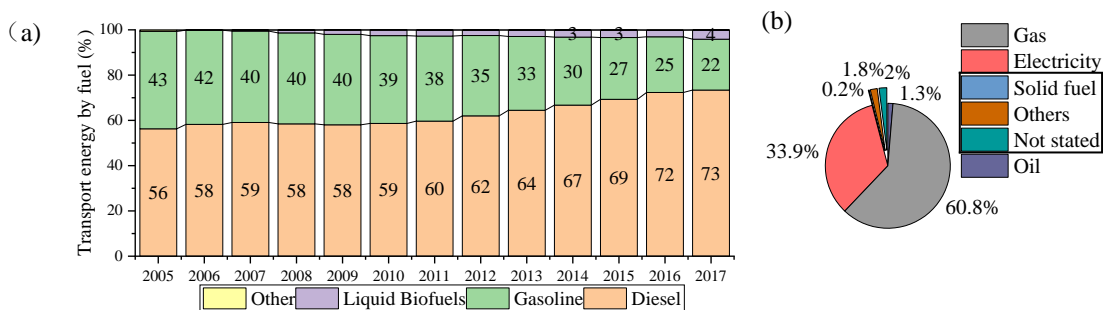
490

Figure 5. The diurnal cycle of organic aerosol (OA) factors, including Hydrocarbon-like OA (HOA), cooking (COA), peat, coal, wood, and oxygenated OA (OOA) during P1 and P2 at the kerbside (a, c) and residential site (b, d).



495

Figure 6. Box plots of the of submicron organic aerosol (OA), sulfate (SO_4), nitrate (NO_3), ammonium (NH_4), black carbon (BC), and NO_x during P1 and P2 at the kerbside and residential site. The median, the 25th and 75th percentiles are represented by the middle, lower and upper vertical bars, respectively. The min and the max percentiles are the bottom and top whiskers, respectively. Note that the time resolution for the ACSM at the kerbside was 5 min while it was 1 h at the residential site, and the time resolution was 1 min for the BC measurement at the kerbside while it was 5 min for the residential site.



500

Figure 7. Contribution of diesel, gasoline, liquid biofuels and other fuels (a) to the total on-road transport energy in Ireland from 2005 and 2017 (SEAI, 2018) and the fraction of the households (b) that claimed to use natural gas, electricity, oil, solid fuels, others, and not stated in Dublin in 2016 (CSO, 2016). Solid fuel, *Others* and *Not stated* are highlighted to show the small fraction of households that are likely to use solid fuels for heating.